The Immunogenomic Landscape of and Immune Cell Infiltration in Bladder Cancer

Zeyu Yang (2286124078@qq.com)
Department of Urology, Changhai Hospital affiliated with Second Military Medical University, Changhai Road 168, Yangpu District, Shanghai 200433, China https://orcid.org/0000-0001-6128-6063

Tianjing Du
Changhai Hospital

Qiao Xiong
Changhai Hospital

Weiwei Zhang
Haisong Hospital

Chao Wang
Haisong Hospital

Longqing Xiang
Haisong Hospital

Shuxiong Zeng
Changhai Hospital

Chuanliang Xu
Changhai Hospital

Research

Keywords: Bladder cancer, immune cell infiltration, immune-related genes, prognostic factor, The Cancer Genome Atlas

Posted Date: August 18th, 2020

DOI: https://doi.org/10.21203/rs.3.rs-55393/v1

Abstract

Background

The role of immune cell infiltration in tumor biology and the potential of immunotherapy for the treatment of several cancers have been proven. However, the immunogenomic landscape and immune cell infiltration need to be comprehensively analyzed in bladder cancer (BC). This study aimed to explore the immune-related genes (IRGs) in BC to create a prognostic risk assessment model and gain some insights into the molecular underpinnings of BC.

Methods

Based on the datasets retrieved from The Cancer Genome Atlas (TCGA) database, we identified survival-associated IRGs via univariate Cox analysis. Then, we created an immune-related gene-based prognostic factor (IRGPF) and validated it by multivariable Cox analysis. We displayed the profiles of 22 types of immune cells by using CIBERSORT and explored the relationship between IRGs and immune cell infiltration.

Results

Altogether, 58 differentially expressed IRGs were found to be associated with the prognosis of patients with BC. We constructed a prognostic assessment model as an IRGPF with IRGs (*THBS1*, *CXCL9*, *CXCL11*, *FABP6*, *BIRC5*, and *PPY*). Profiles of the infiltrating immune cells confirmed their significance based on clinical factors and individual differences. The IRGPF was related to immune cell infiltration, and the key gene was identified as *THBS1*.

Conclusions

Our findings confirmed that IRGs could act as independent prognostic factors and immune-driver factors. Patients with high levels of activated memory CD4 T cells but low levels of resting memory CD4 T cells had a better prognosis. This study indicates the possibility of developing new immunotherapeutic strategies and individualized treatment based on this approach.

Background

In 2020, it is estimated that approximately 81,400 people will be newly diagnosed with bladder cancer (BC), with approximately 17,980 deaths, in the United States [1]. BC is a highly prevalent disease and is related to substantial and increasing morbidity and mortality; its management requires long-term follow-up, as well as expensive and complex therapeutic strategies [2, 3]. Nearly 50% of the patients with BC are in an advanced stage with poor prognosis when diagnosed [4]. Furthermore, distant recurrence still

occurs in approximately 50% of patients with muscle-invasive BC after radical cystectomy, which mostly occurs in lymph nodes, lungs, liver, and bone within 24 months [4, 5]. Therefore, it is crucial to explore the pathogenesis and molecular classification of BC to develop better therapeutic approaches.

In recent years, immunotherapy has been applied to and recognized for the treatment of various cancers, and this has been a main driver of personalized therapy [6–8]. Therapies that target immune checkpoints, such as programmed cell death protein 1, programmed cell death ligand 1, and cytotoxic T lymphocyte-associated antigen 4, are regarded as promising for BC [9]. In addition, some studies have revealed that immune cell infiltration is related to clinical characteristics, such as tumor stage, grade, and prognosis, whereas clusters based on immune cell infiltration are conducive to the selection of treatment strategies [10–12]. Moreover, immune-related genes (IRGs) were integrated to construct an independent prognostic assessment model for papillary thyroid cancer patients [13]. All these results confirm the significance of immunology and immunotherapy in the treatment of cancers.

However, in BC, only a limited number of studies has analyzed the prognostic significance of IRGs and the correlation between immune cell infiltration and BC outcomes. Such studies might illuminate the probable molecular mechanisms involved in BC, thereby facilitating the development of effective therapeutic strategies. The aim of this study was to explore the IRGs in BC as prognostic assessment tools in the clinic and as a clue to understanding immune cell infiltration. We constructed a prognostic risk assessment model for patients with BC by integrating the survival-associated IRGs and exploring the whole immune cell landscape. We gained insight into the relationship between IRGs and immune cell infiltration to explore the underlying regulatory mechanisms. These results could help to gain a deeper understanding of the independent prognostic factors, novel biomarkers, and molecular mechanisms involved in BC, which could provide significant impetus to the development of unique immunotherapeutic approaches and individualized patient management.

Materials And Methods

Data acquisition

We downloaded the RNASeqV2 normalized count datasets (n = 430), simple nucleotide variation datasets (n = 411), and clinical datasets (n = 409) from The Cancer Genome Atlas (TCGA, https://cancergenome.nih.gov/), all of which were combined into a matrix. We summarized and log-transformed the normalized mRNA expression datasets. A total of 411 data files represented tumor samples, whereas 19 represented normal samples. We extracted the information on age, sex, tumor grade and stage, survival status, and survival time from the clinical data files. Furthermore, we downloaded the GSE31864 dataset from the Gene Expression Omnibus (GEO) database to conduct external validation. We acquired a set of IRGs based on the Immunology Database and Analysis Portal (ImmPort) repository [14]. We identified clinically relevant transcription factors (TFs) from the Cistrome Cancer web resource [15]. All aforementioned data are open-source; hence, no approval of the ethics committee was required.

Differentially expressed genes (DEGs)

To obtain the DEGs, we explored the datasets using R software and edgeR package [16]. A Wilcoxon test was performed to compare the tumor and normal tissues, taking $\log_2$ |fold change| > 1 and a false discovery rate (FDR) < 0.05 as the cut-off values for screening. Differentially expressed immune-related genes (DEIRGs) and TFs were then identified from all DEGs. We applied the Database for Annotation, Visualization, and Integrated Discovery to complete the functional enrichment analysis for DEIRGs to obtain the relevant Gene Ontology terms and visualized the results through the Gopolt R package. An FDR < 0.05 was set as the cut-off value for screening. In addition, functional enrichment analysis based on the Kyoto Encyclopedia of Genes and Genomes (KEGG) pathway database was performed with an adjust p < 0.05 as the cut-off.

Identification of survival-associated IRGs and construction of the regulatory network

We conducted univariate Cox analysis to explore the survival-associated IRGs with p < 0.05 as the cut-off value. The network between TFs and survival-associated IRGs was built using the Pearson test and displayed using Cytoscape software. P < 0.001 and |Cor| > 0.4 were taken as the cut-off values.

Model construction and validation

Using multivariate Cox regression, datasets from TCGA were randomly divided on average into two parts, one as a training cohort for constructing a prognostic risk assessment model and the other as a testing cohort for internal validation. Datasets from the GEO database were used for external validation. All patients were classified into high and low risk groups by using the median risk score of the training cohort. Survival analysis between the two groups was performed using the Kaplan–Meier curves and log-rank test. We utilized the time-dependent receiver operating characteristic (ROC) curve to evaluate the prognostic performance of the testing, training, and validation cohorts.

Immune cell infiltration

By using the CIBERSORT algorithm, we calculated the relative proportions of 22 types of tumor-infiltrating immune cells [17]. We performed this analysis using the CIBERSORT code and R software based on 1000 permutations. We quantified the 22 immune cell types using the CIBERSORT p-value for each sample, through which we removed the deconvolution results with no statistical significance. Samples with a CIBERSORT p-value less than 0.05 were included in the subsequent analysis. Next, the differences in 22 types of infiltrating immune cells between the carcinoma and normal tissues were determined using the Wilcoxon test along with the differences in infiltrating immune cells based on pathological stage and TNM stage. The relationship between tumor-infiltrating immune cells and overall survival (OS) was explored using the Kaplan–Meier curves and evaluated via the log-rank test.

We conducted hierarchical clustering analysis of all included patients to confirm the correlation between the classes and clinical factors. The association between clusters and OS was explored using the Kaplan–Meier curves and assessed by the log-rank test. We conducted a Pearson test to explore the

correlation between the risk score and the infiltrating immune cells. Additionally, the key genes were identified.

Results

Identification of DEGs

A total of 4880 DEGs associated with BC were identified in the TCGA cohort, including 1422 downregulated and 3458 upregulated genes (Figs. 1A and 1D). We selected 259 DEIRGs, including 140 downregulated and 119 upregulated (Figs. 1B and 1E), whereas 77 differentially expressed TFs were extracted, including 41 downregulated and 36 upregulated (Figs. 1C and 1F). Using the gene functional enrichment analysis, DEIRGs were found to be enriched in certain cellular components, biological processes, and molecular functions (Fig. 1G). Moreover, based on the KEGG pathway analysis, DEIRGs were found to be mostly enriched in cytokine–cytokine receptor interactions (Fig. 1H).

Identification of survival-associated IRGs and construction of the regulatory network

The univariate Cox analysis of DEIRGs in BC showed that 58 genes were associated with OS ($p < 0.05$, Fig. 2). The survival-associated IRGs were mostly enriched in categories such as extracellular region, extracellular space, growth factor activity, inflammatory response, and positive regulation of cell proliferation (Fig. 1I). By using the correlation test, we developed a regulatory network consisting of 27 TFs and 33 survival-associated IRGs ($|cor| > 0.4$, $p < 0.001$; Fig. 1J).

Construction and validation of the prognostic risk model

We constructed a prognostic risk-assessment model based on the training cohort using multivariate Cox regression analysis (Fig. 3A). The risk score was calculated using the following formula: level of *THBS1* expression · 0.006 + level of *CXCL9* expression · (− 0.009) + level of *CXCL11* expression · (− 0.020) + level of *FABP6* expression · (− 0.030) + level of *BIRC5* expression · 0.023 + level of *PPY* expression · (0.466). According to this formula, we calculated the risk score for the testing cohort and the validation cohort. Based on the median risk score for the training cohort, patients were classified into high- and low-risk groups. We found that the patients in the low-risk group had a better 5-year OS than the patients in the high-risk group in all cohorts (Fig. 3B–D). We used time-dependent ROC curves to evaluate the prognostic risk assessment model, and calculated the area under the curve values of the training cohort, testing cohort, and validation cohort, which were 0.775, 0.653, and 0.634, respectively (Fig. 3E–G). Then, we showed the level of gene expression integrated based on the risk model (Figure S1A–C), risk score (Figure S1D–F), and survival status (Figure S1G–I) of patients in the high- and low-risk groups in the three cohorts. Using the univariate and multivariate Cox analyses, we showed that the risk score calculated by the model could act as an independent prognostic factor for BC in the TCGA cohort (Fig. 3H, 3I).

Landscape of IRG mutations and immune cell infiltration

We next explored genetic alterations in survival-associated IRGs and found that missense mutations comprised the most common type of mutation (Fig. 4A). *AHNAK* had the highest mutation rate, at more than 20%. By using the CIBERSORT algorithm, we first depicted 22 subpopulations of immune cells in patients with BC in the TCGA cohort with $p < 0.05$ as a filter (Fig. 4B). The difference in immune cell infiltration between the normal and tumor samples was also explored. Naive B cells, memory B cells, and resting mast cells were found to be decreased in tumor samples, whereas resting NK cells, M0 macrophages, and M1 macrophages were increased ($p < 0.05$; Fig. 4C). The proportions of different infiltrating immune cells were weakly to moderately correlated (Figure S2A). In addition, M0 macrophages were found to be related to lymph node metastasis and distant metastasis ($p < 0.05$; Figure S2B and 2F), and M2 macrophages were found to be related to distant metastasis ($p < 0.05$; Figure S2C). We found that activated memory CD4 T cells were related to the pathological stage and lymph node metastasis ($p < 0.05$; Figure S2D). Survival analysis showed that the high resting memory CD4 T cell infiltration group had a worse 5-year OS ($p < 0.05$; Figure S2G). In contrast, the high resting NK cell infiltration group had a better 5-year OS ($p < 0.05$; Figure S2H).

Clustering analysis of immune cell infiltration

Given that the variation in the proportions of infiltrating immune cells might be an intrinsic feature that could characterize the individual differences, we performed hierarchical clustering analysis to further explore the relationship between immune cell infiltration and the clinical outcome of BC. The optimal number of clusters was determined as suggested, and appeared to be $k = 3$. This was an adequate selection with clustering stability increasing from $k = 2$ to 9 in TCGA datasets (Fig. 5A and B). The consensus matrix heatmap revealed the three identified clusters, each of which appeared as well-individualized clusters (Fig. 5C). Furthermore, clusters were correlated with the distinct patterns of OS (Fig. 5D). The relationships between the cell proportions of each cluster and clinical factors showed that cluster 1, with high levels of CD8 T cells and activated memory CD4 T cells but low levels of resting memory CD4 T cells, was associated with better prognosis (Fig. 5E).

Correlation analysis between the IRGPF and immune cell proportions

We finally analyzed the relationship between the IRGPF and immune cell infiltration ($p < 0.05$; Fig. 6). The risk score was positively related to the infiltration of M0 macrophages, M2 macrophages, resting mast cells, and neutrophils (Fig. 6A–D). In contrast, the risk score was negatively related to M1 macrophages, resting NK cells, activated CD4 memory T cells, CD8 T cells, and follicular helper T cells (Fig. 6E–I).

Moreover, we explored the relationship between the key gene, *THBS1* and immune cell infiltration ($p < 0.05$; Figure S3). The risk score was positively related to the infiltration of neutrophils, resting mast cells,

and M2 macrophages (Figure S3A–C). In contrast, the risk score was negatively related to the follicular helper T cells, regulatory T cells, CD8 T cells, and resting dendritic cells (Figure S3D–G).

Discussion

In recent years, increasing attention has been paid to the treatment of tumors using immunotherapy, and great progress has been made in this field [18–20]. Further, the importance of IRGs in tumor progression and immunotherapeutics has been well proven. Moreover, immune cell infiltration, taken as one of the intrinsic features of the tumor has been confirmed to be related to tumor grade, progression, and prognosis. However, fewer studies concerning IRGs have been conducted for BC, especially with respect to the clinical significance of immune cell infiltration, which might help to elucidate the underlying molecular mechanisms and describe the immune status more comprehensively [10–12].

Prognostication in BC cannot be exact, despite the knowledge that the depth of tumor infiltration into the bladder wall can provide a simple stratification of risk [21–23]. However, integrating multiple biomarkers into a single model could substantially improve the prognostic value over that of a single model [24–26]. To create a simple and convenient indicator for assessing the prognosis of patients with BC, we created an IRGPF profile. The IRGs were explored to construct a risk assessment model to predict clinical outcomes. A previous studies lacked validation [27]; however, we conducted external and internal validation to improve the credibility of our findings.

We discovered that some infiltrating immune cells are related to the TNM stage and prognosis in BC. In addition, our cluster analysis results of immune cell infiltration could significantly improve the prognosis of patients. The results confirmed that immune cells are crucial to BC progression, similar to the findings of some previous studies on BC and other cancers, and confirming the importance of immune cells in the pathophysiology of cancer [10–12]. Based on clustering analysis and survival analysis, we found that patients with high levels of activated memory CD4 T cells but low levels of resting memory CD4 T cells had a better prognosis. Further, highly activated CD4 cell infiltration predicted decreased lymphatic metastasis and a lower pathological grade. Activated memory CD4 T cells might play an important role in BC, which helps to discover new therapeutic targets. Our results indicated that the IRGPF was significantly correlated with some infiltrating immune cells, suggesting that it could not only assess prognosis but also indicate the immune status. This might provide clues to the molecular mechanism of immune cell infiltration.

Among the results of these experiments, the *THBS1* gene caught our attention. THBS1 features prominently in the TF-mediated network regulating the survival-associated IRGs. As an independent prognostic factor, *THBS1* played a key role in the development of a prognostic assessment model. Our analysis also confirmed that *THBS1* is related to immune cell infiltration, which we have great interest in exploring further. Some studies suggested that THBS1 is involved in tumor progression and metastasis. THBS1 promotes the invasion of oral squamous cell carcinoma induced by TGFB1 in the cancer stroma [28]. THBS1 is also a prognostic factor and has a negative relationship with histone deacetylase in

advanced gastric cancer [29]. Gene methylation leads to brain metastases of solid tumors, primarily involving epigenetic silencing of THBS1 regulators, such as RB1/p16INK4a [30]. *THBS1* might also participate in the development and progression of BC and could be a potential key gene to reveal the underlying pathogenesis.

Our findings might help to reveal the drivers and mechanisms of immune cell infiltration. However, there are some limitations. First, our proposed model needs more reliable datasets to validate the findings. Second, our molecular results need to be verified by vitro or in vivo experiments. Third, the function of THBS1 in BC development and progression needs further study. A multi-group analysis involving immunogenomics, epigenetics, transcriptomics, metabolomics, and proteomics should be employed to further characterize the molecular mechanisms involved in BC.

Conclusion

We analyzed the significance of IRGs in monitoring the prognosis of BC and the relationship between IRGs and immune cells. We also identified a key gene, *THBS1*, relevant to BC prognosis. We anticipate that the risk assessment prognostic model that we created would be clinically significant. Our findings provide new insights that might shed some light on the pathogenesis of BC and help in the development of new immunotherapeutic strategies.

List Of Abbreviations

BC, bladder cancer; DEGs, differentially expressed genes; DEIRGs, differentially expressed immune-related genes; FDR, false discovery rate; GEO, Gene Expression Omnibus; IRGPF, immune-related gene-based prognostic factor; IRGs, immune-related genes; OS, overall survival; ROC, receiver operating characteristic; TCGA, The Cancer Genome Atlas; TFs, transcription factors

Declarations

Ethics approval and consent to participate

All the data above is open-ended; hence, no approval of the ethics committee was required.Consent was obtained from each participant

Consent for publication

Not applicable.

Availability of data and materials

All the data above is open-ended.

Competing interests

The authors declare that they have no competing interests.

Funding

This research was financed by grants from Shanghai Sailing Program(18YF1422700), Starting Foundation for Young Scientists of Second MilitaryMedical University (2017QN11), National Natural ScienceFoundation of China (81802515).

Authors' contributions

Conception and design: ZYY and TJD

Acquisition of data: ZZY, TJD and QX

Analysis and interpretation of data: ZZY, TJD and QX

Drafting of the manuscript: ZZY and TJD

Reviewed and edited the manuscript: YPX, AWL, ZSZ, CLX, SXZ, LQX, WWZ, CW

Study supervision: CLX, and SXZ

Acknowledgements

Not applicable.

Authors' information

Zeyu Yang, Tianjing Du, and Qiao Xiong contributed equally to this work.

Affilications

Department of Urology, Changhai Hospital affiliated with Second Military Medical University, Changhai Road 168, Yangpu District, Shanghai 200433, China

Zeyu Yang, Qiao Xiong, Yongping Xue, Anwei Liu, Chuanliang Xu, and Shuxiong Zeng

Department of burns and traumas, Changhai Hospital affiliated with Second Military Medical University, Changhai Road 168, Yangpu District, Shanghai 200433, China

Tianjing Du

Department of Urology, Haisong Hosipitial, Songbao Road 196, Baoshan District, Shanghai, China

Longqing Xiang, Chao Wang, Weiwei Zhang.

Corresponding author

Correspondence toChuanliang Xu and Shuxiong Zeng

References

1. Siegel RL, Kimberly MM, Miller D. and D.P. Ahmedin Jemal, Cancer statistics, 2020. CA-A CANCER JOURNAL FOR CLINICIANS, 2020. 70(1): p. 7–30.
2. Comperat E, et al. A practical guide to bladder cancer pathology. Nature reviews Urology. 2018;15(3):143–54.
3. Woldu SL, et al. Validating the predictors of outcomes after radical cystectomy for bladder cancer. Cancer. 2019;125(2):223–31.
4. Bokarica P, Hrkac A, Gilja I, Re: J, Alfred Witjes T, Lebret EM, Comperat, et al. Updated 2016 EAU Guidelines on Muscle-invasive and Metastatic Bladder Cancer. Eur Urol 2017; 71: 462 – 75. European urology, 2017. 72(2): p. E45-E45.
5. Sanli O, Lotan Y. Current approaches for identifying high-risk non-muscle invasive bladder cancer. Expert Rev Anticancer Ther. 2018;18(3):223–35.
6. Popovic A, Zaidi N, Jaffee EM. Emerging strategies for combination checkpoint modulators in cancer immunotherapy. The Journal of Clinical Investigation: The Official Journal of the American Society for Clinical Investigation. 2018;128(8):3209–18.
7. Rai V, et al. Cellular and molecular targets for the immunotherapy of hepatocellular carcinoma. Molecular Cellular Biochemistry: An International Journal for Chemical Biology. 2018;437(1/2):13–36.
8. Johnson CE, Hargadon KM, Williams CJ. Immune checkpoint blockade therapy for cancer: An overview of FDA-approved immune checkpoint inhibitors. Int Immunopharmacol. 2018;62(1):29–39.
9. Lerner SP. Summary and Recommendations from the National Cancer Institute's Clinical Trials Planning Meeting on Novel Therapeutics for Non-Muscle Invasive Bladder Cancer. Bladder Cancer. 2016;2(1):165–202. 1).
10. Fu H, et al. Identification and Validation of Stromal Immunotype Predict Survival and Benefit from Adjuvant Chemotherapy in Patients with Muscle-Invasive Bladder Cancer. Clin Cancer Res. 2018;24(13):3069–78.
11. Ali HR, et al. Patterns of Immune Infiltration in Breast Cancer and Their Clinical Implications: A Gene-Expression-Based Retrospective Study. PLOS Medicine. 2016;13(12):e1002194.
12. Xiong Y, et al. Profiles of immune infiltration in colorectal cancer and their clinical significant: A gene expression-based study. Cancer Med. 2018;7(9):4496–508.
13. Lin P, et al. Development of a prognostic index based on an immunogenomic landscape analysis of papillary thyroid cancer. Aging. 2019;11(2):480–500.
14. RImmPort. an R/Bioconductor package that enables ready-for-analysis immunology research data. Bioinformatics. 2017;33(7):1101–3.

15. Mei S, et al., Cistrome Cancer: AWeb Resource for Integrative Gene Regulation Modeling in Cancer. Cancer research: The official organ of the American Association for Cancer Research, Inc, 2017. 77(21): p. E19-E22.
16. McCarthy DJ, Smyth GK, Robinson MD. edgeR: a Bioconductor package for differential expression analysis of digital gene expression data. Bioinformatics. 2010;26(1):139–40.
17. Chen B, et al. Profiling Tumor Infiltrating Immune Cells with CIBERSORT. Methods Mol Biol. 2018;1711:243–59.
18. Guven DC, et al. Gut microbiota and cancer immunotherapy: prognostic and therapeutic implications. Future Oncol. 2020;16(9):497–506.
19. Turbitt WJ, et al., Obesity and CD8 T cell metabolism: Implications for anti-tumor immunity and cancer immunotherapy outcomes. Immunol Rev, 2020.
20. Balan V, Wang J, The CRISPR System and Cancer Immunotherapy Biomarkers. Methods Mol Biol, 2020. 2055: p. 301–322.
21. Sanli O, et al. Bladder cancer. Nat Rev Dis Primers. 2017;3:17022.
22. Yikilmaz TN, et al. Clinical Use of Tumor Markers for the Detection and Prognosis of Bladder Carcinoma: A Comparison of CD44, Cytokeratin 20 and Survivin. Urol J. 2016;13(3):2677–83.
23. Wang Y, et al. Novel Biomarkers Associated With Progression and Prognosis of Bladder Cancer Identified by Co-expression Analysis. Front Oncol. 2019;9:1030.
24. Zhang JX, et al. Prognostic and predictive value of a microRNA signature in stage II colon cancer: a microRNA expression analysis. Lancet Oncol. 2013;14(13):1295–306.
25. Vander Hoeven JJ. 70-Gene signature as an aid to treatment decisions in early-stage breast cancer. Ned Tijdschr Geneeskd. 2017;161:D1369.
26. Halabi S, et al. Prognostic model predicting metastatic castration-resistant prostate cancer survival in men treated with second-line chemotherapy. J Natl Cancer Inst. 2013;105(22):1729–37.
27. Li B, et al. Development and Validation of an Individualized Immune Prognostic Signature in Early-Stage Nonsquamous Non-Small Cell Lung Cancer. JAMA Oncol. 2017;3(11):1529–37.
28. Pal SK, et al. THBS1 is induced by TGFB1 in the cancer stroma and promotes invasion of oral squamous cell carcinoma. Journal of Oral Pathology Medicine. 2016;45(10):730–9.
29. Eto S, et al. The Relationship of CD133, Histone Deacetylase 1 and Thrombospondin-1 in Gastric Cancer. Anticancer Research: International Journal of Cancer Research Treatment. 2015;35(4):2071–6.
30. Gonzalez-Gomez P, et al. Promoter methylation status of multiple genes in brain metastases of solid tumors. Int J Mol Med. 2004;13(1):93–8.

Figures

Figure 1

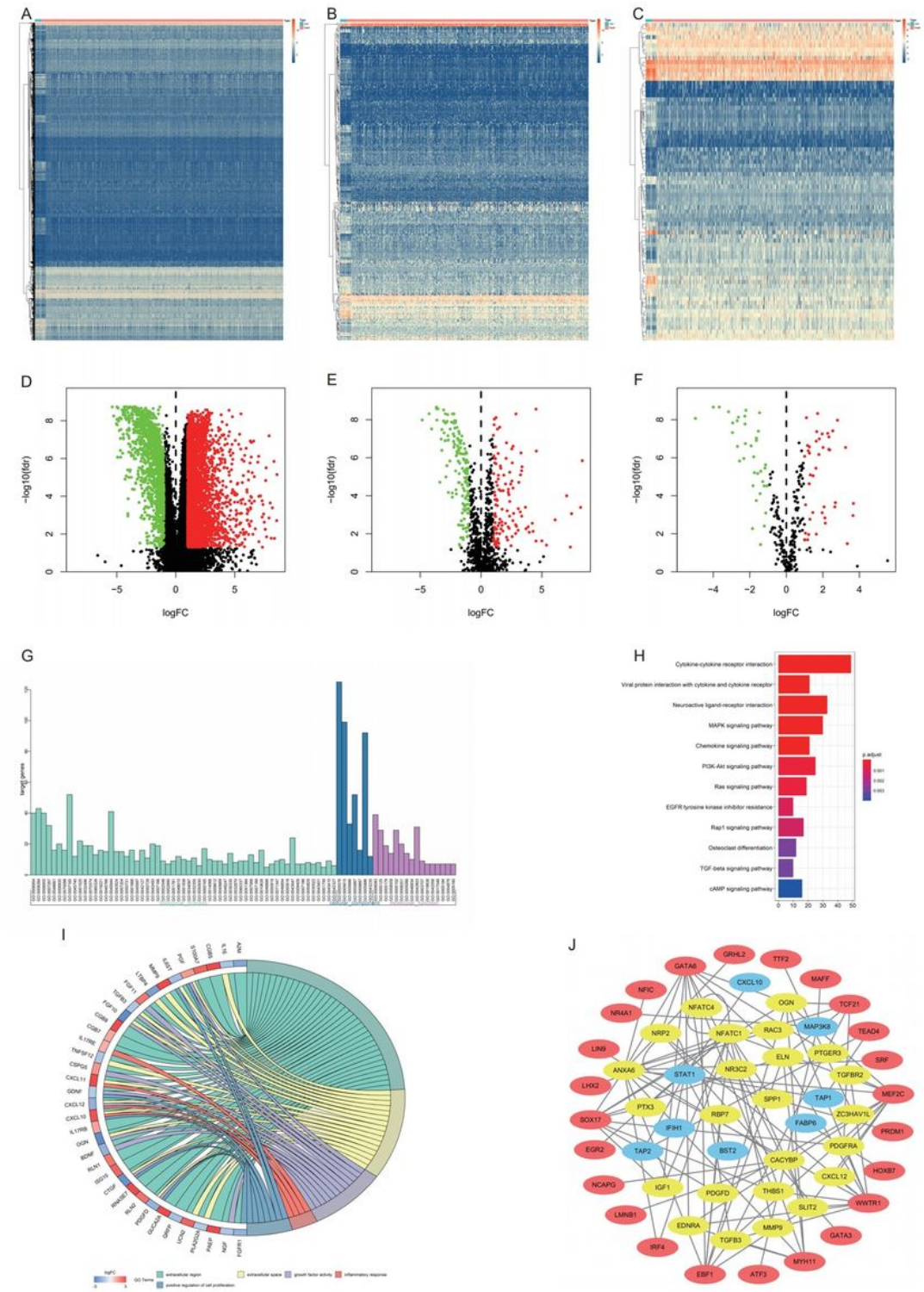

Figure 1

Differentially expressed immune-related genes. Heatmap (A) and volcano plot (D) demonstrating the differentially expressed genes between bladder cancer (BC) and normal tissues. Differentially expressed immune-related genes (IRGs) are indicated in the heatmap (B) and volcano plot (E). Differentially expressed transcription factors (TFs) are revealed in the heatmap (C) and volcano plot (F). In the heatmaps, bluerepresents downregulation, redrepresents upregulation, and yellowrepresents similar

expression levels. In the volcano plots, red dots represent upregulated genes, green dots represent downregulated genes, and black dots represent undifferentiated genes.(G) Enrichment analysis of the biological process, molecular function, and cellular component categories based on Gene Ontology (GO) analysis of differentially expressed IRGs. (H) The significant Kyoto Encyclopedia of Genes and Genomes (KEGG) pathways according to the enrichment analysis of differentially expressed IRGs. (I) Survival-associated IRGs significantly enriched in the different GO terms. (J) The network between differentially expressed TFs and the IRGs associated with BC prognosis.

Figure 2

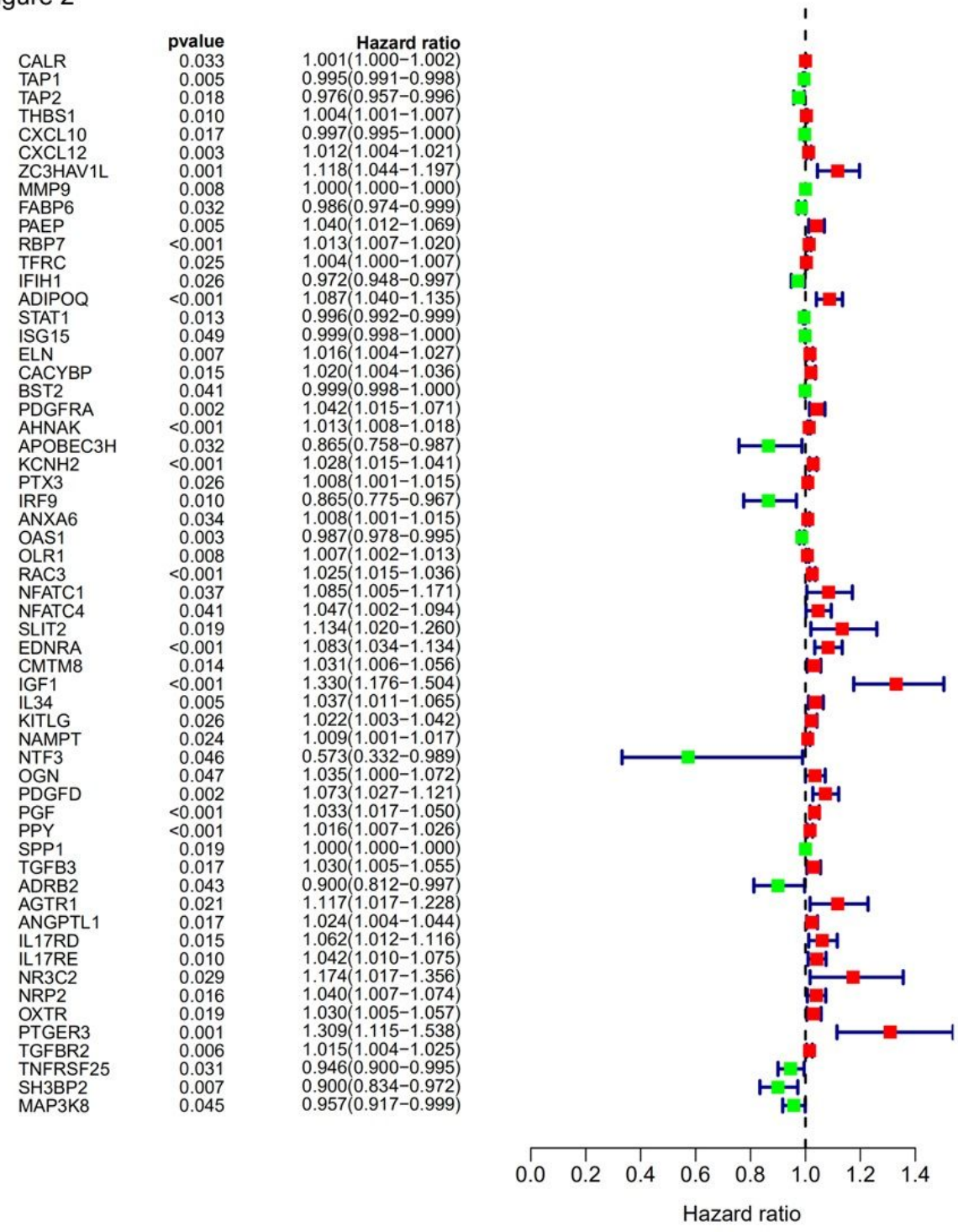

Figure 2

Differentially expressed immune-related genes (IRGs)associated with overall survival (OS) using univariate Cox regression analysis.

Figure 3

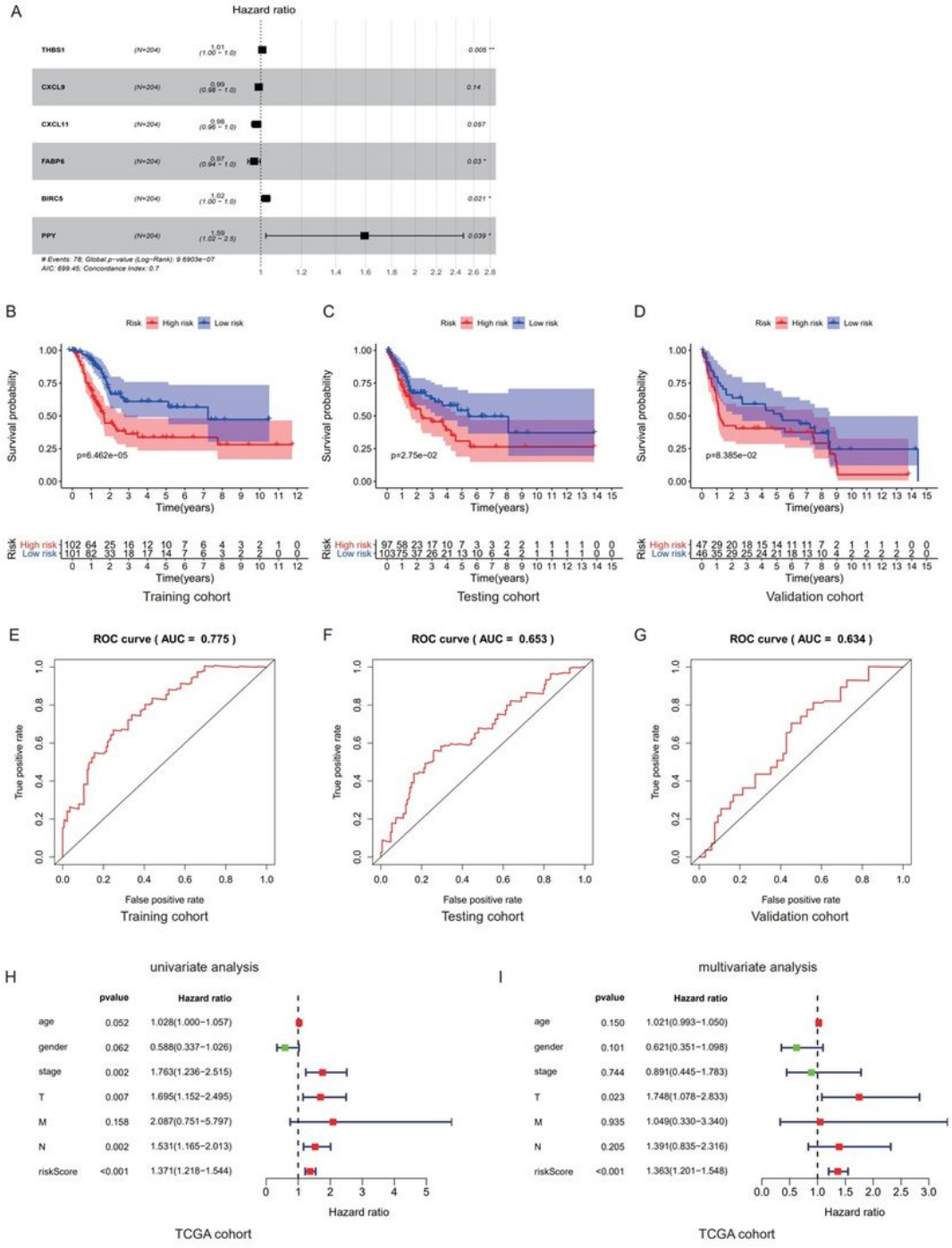

Figure 3

Construction of the prognostic index model based on immune-related genes (IRGs). (A) Six IRGs used in building the prognostic indexmodel as calculated by multivariate Cox regression.(B–D) Kaplan–Meier overall survival (OS) curves for patients in the training cohort, testing cohort, and validation cohort.Samples were assigned to high-risk and low-risk groups based on the risk score. (E–G) Survival-dependent receiver operating characteristic (ROC) curve validation of the prognostic value of the prognostic indexmodel in the training cohort, testing cohort, and validation cohort. Forest plots (H and I) reveal univariate and multivariateCox regression analysisresults based on the risk score and clinical factors.

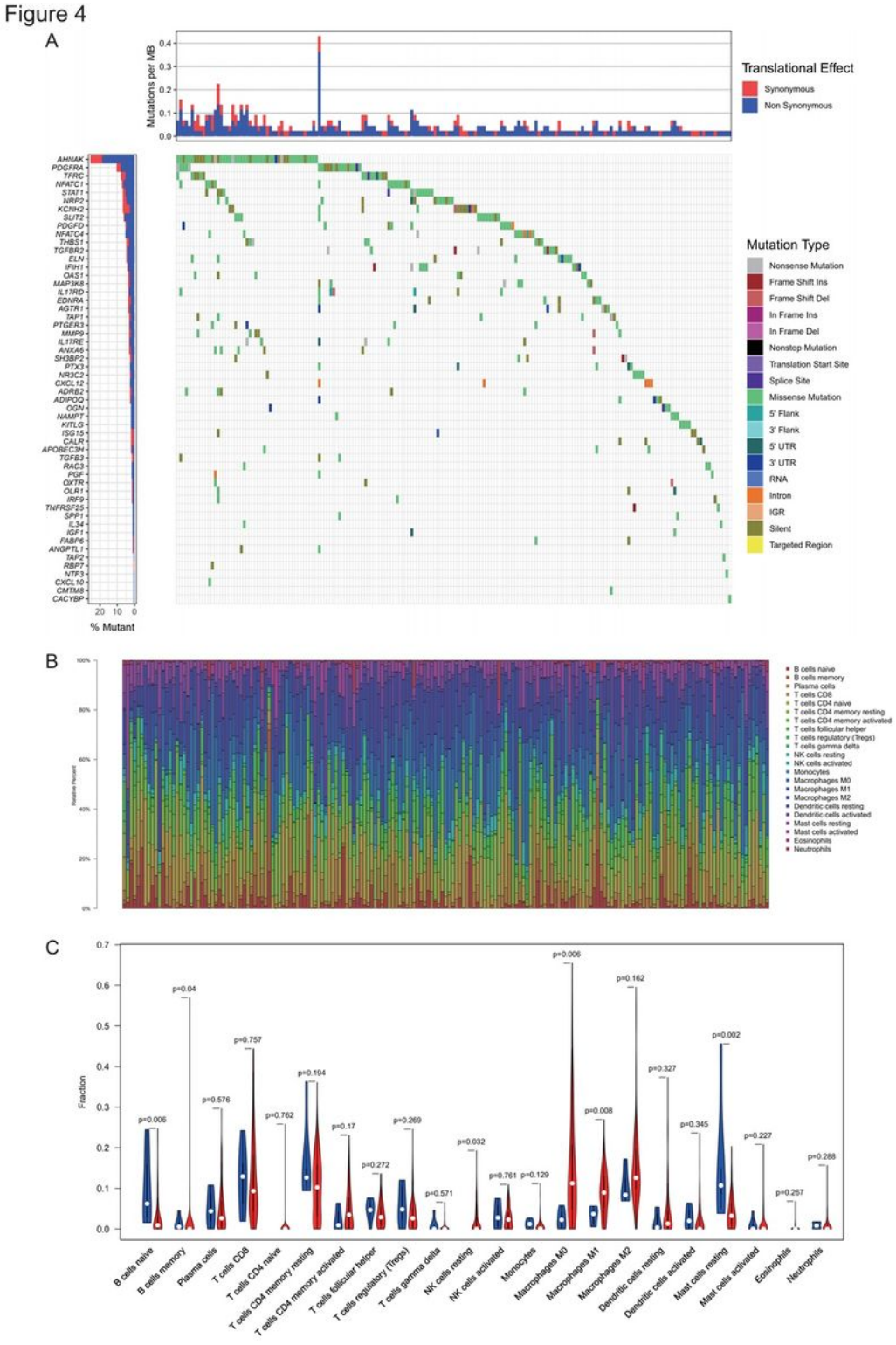

Figure 4

Landscape of immune-related genes (IRG)mutations and immune cell infiltration in BC.Waterfall plots (A) show the mutation landscape of IRGs associated with bladder cancer (BC) prognosis. (B) Twenty-two immune cell proportions of samples in the TCGA cohort. (C) The difference in immune cell infiltration between BC and normal tissues.

Figure 5

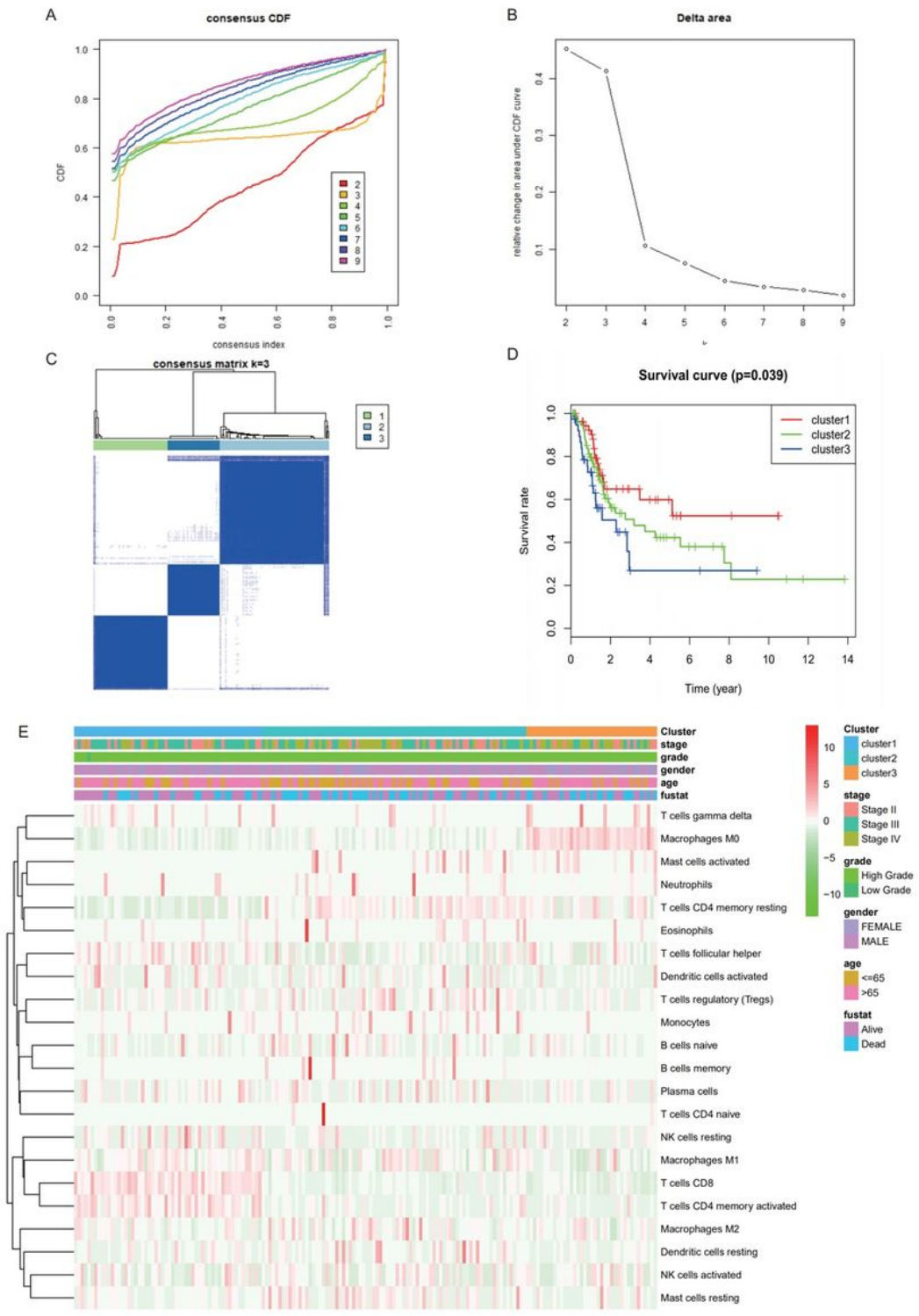

Figure 5

Clustering analysis of immune cells in bladder cancer (BC). (A) Consensus clustering cumulative distribution function (CDF) for k = 2 to 9. (B) Relative change in area under the CDF curve for k = 2 to 9. (C) Consensus matrix heatmap defining the three clusters of samples. (D) Kaplan–Meier overall survival (OS) curves of different clusters. (E) Heat map of immune cell infiltration in three clusters.

Figure 6

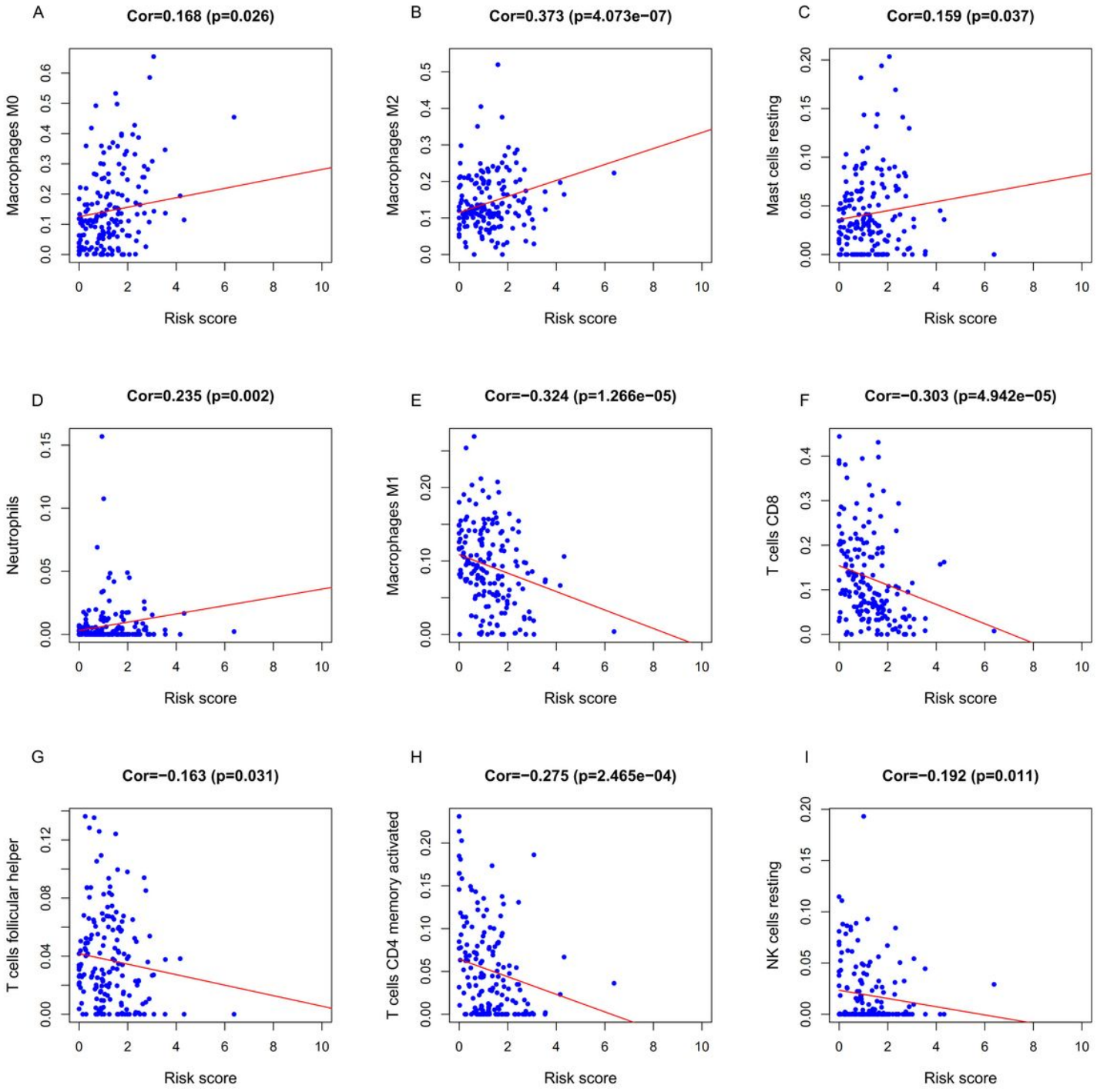

Figure 6

Relationship between the IRGPF andimmune cell proportions with statistical significance (P < 0.05).(A) M0 macrophages; (B) M1 macrophages; (C) M2 macrophages; (D) resting mast cells; (E) neutrophils; and (F) resting NK cells; (G) activated memory CD4 T cells; (H) CD8 T cells; (I) follicular helper T cells. IRGPF,immune-related gene-based prognostic factor.

Supplementary Files

This is a list of supplementary files associated with this preprint. Click to download.

- figureS2.tif
- figureS1.tif
- figureS3.tif